Hydrogen Bond Type Contributions to the Anomeric Effect in S−C−P(O) and S−C−P(S) Segments†

Gabriel Cuevas*

Contribution from the Instituto de Química, Universidad Nacional Autónoma de México, Cd. Universitaria, Apdo. Postal 70213, 04510 Coyoacán México, D.F., México

Received September 5, 1997. Revised Manuscript Received November 12, 1999

Abstract: Ab initio B3LYP/6-31G(*d,p*) within the frame of Density Functional Theory was used to calculate the relative energies of the rotamers in the axial and equatorial chair conformations of 2-dimethylposphinoyl-1,3-dithiane and gauche-anti conformations of dimethylphosphinoyl(methylsulfanyl)methane. The theoretical energy differences and geometric patterns are similar to those determined experimentally for the diphenylphosphinoyl analogue. The electrostatic nature of hydrogen bonds in the title molecules studied was analyzed through the Topological Theory of Atoms in Molecules (AIM). The bonding paths C−H···X−P (X = O, S), as well as the properties of the critical points associated with them at the B3LYP/6-31G(*d,p*)//(BP+NLSCF)/DZVP2 level of theory, are described. The characterization of the H−X (X = O, S) bond path is relevant because it allows one to establish that interactions of the hydrogen-bond type can make a stabilizing contribution to the axial and gauche preferences of the segments studied here. From the results of this paper, it is clear that the AIM method is suitable for the study of the interaction between a small polarity C−H donor and a good acceptor, such as the oxygen or sulfur atom bonded to phosphorus.

Introduction

The origin of the anomeric effect in 2-diphenylphosphinoyl-1,3-dithiane (DPP-DT) (Figure 1) had remained obscure up until now.[1] The anomeric effect was found in this system, for the first time, by Juaristi et al.[2] in 1982.

The participation of $n_S \rightarrow \sigma^*_{C-P}$ stereoelectronic interaction is unable to explain the axial conformational preference arising from the well-known low donor capability of the sulfur atom (Figure 2).[3] However, such a stereoelectronic interaction would cause a shortening of the C_2-S bond and a concomitant elongation of the C−P bond in the axial conformer; and this is in contradiction to X-ray geometry of the axial conformer of DPP-DT.[4]

The phosphoryl group in the axial conformer is forced into close proximity to the syn-axial hydrogens, e.g. O···H(4,6-ax) = 2.46 Å[1b] due to the Coulombic interaction between the partially negative phosphoryl oxygen and the slightly positive axial hydrogens at $C_{4,6}$. This electrostatic interaction provides an alternative rationalization of the experimental findings.[1a,5] Nevertheless, substantial experimental data including a very recent microwave study[5c] do not provide support for the aforementioned rationalization. The long-standing controversy

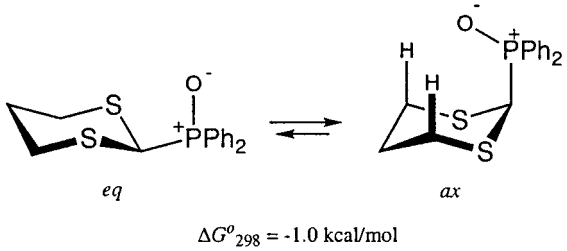

Figure 1.

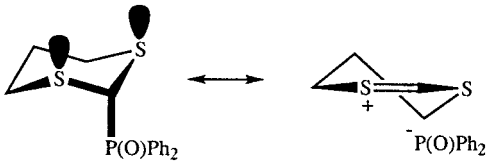

Figure 2. Double bond−no bond hybrid.

on the existence of the C−H···O hydrogen bond has been resolved now.[6,7] The potential of the C−H groups as proton donors in hydrogen bonding originally proposed by Glasstone[8] has been experimentally corroborated. This was accomplished by means of neutron diffraction of a large number of molecules which manifest C−H bonds in intermolecular contacts with oxygen atoms resulting in CH···O hydrogen bonds.[9]

On the other hand, very recent studies[10] on the nature of P−O bond in phosphine oxides clearly suggest the absence of conventional multiple bonds.[11] Atoms in molecules (AIM) studies[12] indicate one highly polarized σ bond in which the

† Contribution No. 1708 of the Instituto de Química UNAM.

(1) (a) Juaristi, E.; Cuevas, G. *The Anomeric Effect*; CRC Press: Boca Ratón, 1995; Section 7.3. (b) Juaristi, E.; Valenzuela, B. A.; Valle, L.; McPhail, A. T. *J. Org. Chem.* **1984**, *49*, 3026.

(2) Juaristi, E.; Valle, L.; Mora-Uzeta, C.; Valenzuela, B. A.; Joseph-Nathan, P.; Fredrich, M. F. *J. Org. Chem.* **1982**, *47*, 5038.

(3) Schleyer, P. V. R.; Jemmis, E. D.; Spitznagel, G. W. *J. Am. Chem. Soc.* **1985**, *107*, 6369.

(4) Juaristi, E.; Valle, L.; Valenzuela, B. A.; Aguilar, M. A. *J. Am. Chem. Soc*. **1986**, *108*, 2000.

(5) (a) Mikolajczyk, M.; Balczewski, P.; Wroblewski, K.; Karolak-Wojciehowska, J.; Miller, A.; Wieczorek, M. W.; Antipin, M. Y.; Struchkov, Y. T. *Tetrahedron* **1984**, *40*, 4885. (b) Mikolajczyk, M.; Graczyk, P.; Wieczorek, M. W. *J. Org. Chem.* **1994**, *59*, 1672. (c) Graczyk, P.; Mikolajczyk, M.; Plass, M.; Kolbe, A., *J. Mol. Struct.* **1997**, *416*, 179.

(6) Taylor, R.; Kennard, O. *J. Am. Chem. Soc.* **1982**, *104*, 5063.

(7) Desiraju, G. R. *Acc. Chem. Res.* **1991**, *24*, 290.

(8) Glasstone, S. *Trans. Faraday. Soc.* **1937**, *33*, 200.

(9) Donohue, J. In *Structural Chemistry and Molecular Biology*; Rich, A., Davison, N., Eds.; W. H. Freeman: San Francisco, 1968; pp 459−463.

(10) Chesnut, D. B. *J. Am. Chem. Soc.* **1998**, *120*, 10504.

10.1021/ja9731231 CCC: $19.00
Published on Web 01/19/2000

strength depends on electrostatic interactions between phosphorus and oxygen. From the studies of Dobado et al.,[12] it is clear that there is no π back-donation from the oxygen to phosphorus atom; and the larger charge at the oxygen atom would favor hydrogen−oxygen electrostatic interactions in the axial conformer (Figure 1), resulting in a CH···O hydrogen bond.

The anomeric effect has been widely studied from a theoretical point of view.[13] The nature of hydrogen bonding was studied theoretically by Bader et al. in 1987.[14] Because these bonds are the result of two closed-shell system interactions, the Laplacian of ρ reflects the properties of the charge distribution. When $\nabla^2\rho(r) > 0$, the value of the charge density at the ρ point is less than the average value of $\rho(r)$ over all neighboring points in space.[15] In this sense, H···O and N···H hydrogen bonds are characterized, according to the AIM theory, by the presence of a bond path and its associated virial path that provide a universal indicator of bonding between the atoms so linked.[16]

Recently, it was suggested that total charge density is a useful tool to confirm hydrogen bonding without invoking charge density.[17] However, local properties such as topology, Laplacian at the bond critical point, and mutual penetration of hydrogen and acceptor atoms as well as integrated properties such as change in charge of bonded hydrogen atoms, energy of destabilization, decrease of dipolar polarization, and the decrease of atomic volume of hydrogen atoms can also be used. From a computational point of view, the second kind, i.e., integrated properties, are more expensive to calculate than local ones, and are worthless since they only confirm the results. Cioslowski[18] has rigorously described the topology of several molecules affected by weak interactions, showing that topological properties are good enough to study these kinds of interactions.

In this paper, ab initio B3LYP/6-31G(*d*,*p*) calculations were performed to calculate the relative energies of the rotamers in the axial and equatorial conformations of 2-dimethylphosphinoyl-1,3-dithiane (DMP-DT) and gauche-anti conformations of dimethylphosphinoyl(methylsulfanyl)methane (DMP-MSM). The Atoms in Molecules Theory (AIM) was applied to perform the topological analysis of the electron density of axial and gauche conformers of both compounds. Indeed, the P−O···H−C hydrogen bond interaction contributes to the stabilizing anomeric effect in the S−C−P(O) segment.

Computational Methods

The full geometry optimization of all structures was solved by using the Density Functional Theory (DFT). We used Becke's exchange functional[19] as well as Perdew's correlation energy functional[20] (BP), with exchange and local correlation according to Vosko et al.,[21] in a self-consistent field calculation. A double-ζ valence plus polarization basis set (DZVP2) was used. These calculations were made on a Cray-Y-MP4/464 supercomputer on a Dgauss 1.1 program.[22]

Single-point calculations were performed at the B3LYP/6-31G(*d*,*p*)//(BP+NLSCF)/DZVP2 level, and from the G92 program[23] wave function archive. The AIMPAC[24] set of programs were used, obtaining the properties of atoms and critical points (cps) in the charge density: density (ρ), Laplacians ($\nabla^2\rho$), and ellipticities (ϵ). Frequency calculations and thermochemical analysis were performed with the G94 program,[24] with full optimized geometries at B3LYP/6-31G(*d*,*p*).

Two of the most important contributions of the AIM theory are the following: the precise definition of an atom in a molecule and the definition of the chemical bond. These concepts correspond to the topological properties of the electron density.[14−16,25] The chemical structure of a molecule is unambiguously described determining the critical points through the electron density, and corresponds to the gradient zero-density points.[26−29] These points, as well as the first and second derivates, can be determined with the use of the PROAIM[24] program. From the second derivate, it is possible to determine the three principal curvatures associated with a critical point due to its index (the algebraic addition of the curvature sign).[26]

A negative curvature implies that the density (ρ) is in a maximum at that point. ρ's gradient is a vector directed toward ρ increase. If a succession of points is calculated where each new point is determined by the previous point, a high charge density path is obtained. This path normally ends in a nucleus, but if there is a nucleus close to the first one, there is necessarily a demarcation surface between them, and the paths are forced to end in a critical point (3,−1). This means that there has to be a surface where $\rho(r)$ is a maximum in a critical point, with two negative curvatures. The positive curvature of this critical point is associated with the axis, perpendicular to the interatomic surface, in which $\rho(r)$ is a minimum. This axis defines the initial direction of two $\nabla\rho$ paths that originates in this critical point and ends in the nucleus. This line of maximal density with respect to the gradient paths is called the bonding path. According to Bader,[16,26] "the existence of a bonding path is a necessary condition and is enough for the existence of a bond".[27,29]

The presence of a bond path and its associated virial path provides a universal indicator of bonding between the atoms so linked. Since weak interactions are primarily the result of a correlation of the electron motions on the two interacting species, their description requires the use of densities obtained from correlated wave functions, determined in an exact manner by DFT methods.[16]

Besides density, ellipticity is an important property of a critical point. This is defined as the coefficient of the negative curves along the

(11) Chesnut, D. B.; Savin, A. *J. Am. Chem. Soc.* **1999**, *121*, 2335. Reed, A. E.; Schleyer, P. v. R. *J. Am. Chem. Soc.* **1990**, *112*, 1434. Wallmeir, H.; Kutzelningg, W. *J. Am. Chem. Soc.* **1979**, *101*, 2804. Rai, U. S.; Symons, M. C. R. *J. Chem. Soc., Faraday Trans.* **1994**, *90*, 2649. Streitwieser, A., Jr.; Rajca, A.; McDowell, R. S.; Glaser, R. *J. Am. Chem. Soc.* **1987**, *109*, 4184. Streitwieser, A., Jr.; McDowell, R. S.; Glaser, R. J. *J. Comput. Chem.* **1978**, *8*, 788.

(12) Dobado, J. A.; Martinez-Garcia, H.; Molina, J. M.; Sundberg, M. R. *J. Am. Chem. Soc.* **1998**, *120*, 8461.

(13) Reference 1a, Chapter 3. Juaristi, E.; Cuevas, G. *Tetrahedron* **1999**, *55*, 359. Freeman, F.; Phornvoranunt, A.; Hehre, W. *J. Phys. Org. Chem.* **1998**, *11*, 831.

(14) Bader, R. F. W.; Carroll, M. T.; Cheeseman, J. R.; Chang, C. *J. Am. Chem. Soc.* **1987**, *109*, 7968.

(15) Bader, R. F. W.; Essen, H. *J. Chem. Phys.* **1984**, *80*, 1943.

(16) Bader, R. F. W. *J. Phys. Chem. A* **1998**, *102*, 7314.

(17) Koch, U.; Popelier, P. L. A. *J. Phys. Chem A* **1995**, *99*, 9747.

(18) Cioslowski, J.; Mixon, S. T. *J. Am. Chem. Soc.* **1992**, *114*, 4382. Cioslowski, J.; Mixon, S. T.; Edwards, W. D. *J. Am. Chem. Soc.* **1991**, *113*, 1083.

(19) Becke, A. D. *Can. J. Chem.* **1988**, *66*, 1052. Becke, A. D. *Phys. Rev. A* **1988**, *38*, 3098.

(20) Perdew, J. P. *Phys. Rev. Lett.* **1985**, *55*, 1665.

(21) Vosko, S. H.; Wilk, L.; Nusair, M. *Can. J. Phys.* **1980**, *58*, 1200.

(22) Cf.: Andzelm, J.; Wimmer, E. *J. Chem. Phys.* **1992**, *96*, 1280. Andzelm, J. In *Density Functional Methods in Chemistry*; Labanowski, J., Ed.; Springer: New York, 1991; p 155.

(23) Gaussian 92/DFT, Revision G.2. Frisch, M. J.; Trucks, G. W.; Schlegel, H. B.; Gill, P. M. W.; Johnson, B. G.; Wong, M. W.; Foresman, J. B.; Robb, M. A.; Head-Gordon, M.; Replogle, E. S.; Gomperts, R.; Andres, J. L.; Raghavachari, K.; Binkley, J. S.; Gonzalez, C.; Martin, R. L.; Fox, D. J.; Defrees, D. J.; Baker, J.; Stewart, J. J. P.; Pople, J. A. Gaussian, Inc.: Pittsburgh, PA, 1993.

(24) Beigler-Kömig, F. W.; Bader, R. F. W.; Tang, T. H. *J. Comput. Chem.* **1982**, *3*, 317.

(25) Gaussian 94, Revision D.4, Frisch, M. J.; Trucks, G. W.; Schlegel, H. B.; Gill, P. M. W.; Johnson, B. G.; Robb, M. A.; Cheeseman, J. R.; Keith, T.; Petersson, G. A.; Montgomery, J. A.; Raghavachari, K.; Al-Laham, M. A.; Zakrzewski, V. G.; Ortiz, J. V.; Foresman, J. B.; Cioslowski, J.; Stefanov, B. B.; Nanayakkara, A.; Challacombe, M.; Peng, C. Y.; Ayala, P. Y.; Chen, W.; Wong, M. W.; Andres, J. L.; Replogle, E. S.; Gomperts, R.; Martin, R. L.; Fox, D. J.; Binkley, J. S.; Defrees, D. J.; Baker, J.; Stewart, J. P.; Head-Gordon, M.; Gonzalez, C.; Pople, J. A. Gaussian, Inc.: Pittsburgh, PA, 1995.

(26) Bader, R. F. W. *Atoms in Molecules−a quantum theory*; Clerendon Press: Oxford, 1990.

(27) Bader, R. F. W. *Acc. Chem. Res.* **1985**, *18*, 9.

(28) Bader, R. F. W. *Chem. Rev.* **1991**, *91*, 893.

(29) Bader, R. F. W.; Slee, T. S.; Cremer, D.; Kraka, E. *J. Am. Chem. Soc.* **1983**, *105*, 5061.

Scheme 1. Total Energy (TE, hartrees), Relative Total Energy (RTE, kcal/mol), Zero-Point Energy (ZPE, hartrees), Enthalpy (*H*, hartrees), and Entropy (*S*, eu) of C−P Rotamers of Dimethylphosphinoylthiomethylmethane at B3LYP/6-31G(*d*,*p*)

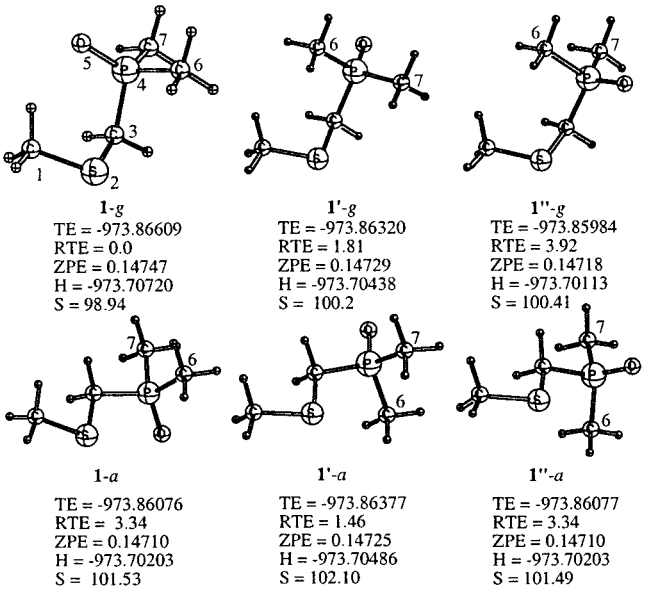

perpendicular axis to the bonding path, $\epsilon = \lambda(1)/\lambda(2) - 1$, and should be considered as an index of bond's anisotropy. If the studied bond belongs to a ring or a cage, two or more of its interatomic surfaces will have critical points (3,+1), called ring critical points, and (3,+3), which is a cage critical point. The Poincare−Hopf relation determines the type of critical points that can coexist in a system. For a number of *n* nucleus associated with *b* bond paths, *r* rings, and *c* cages, the relation establishes:

$$n - b + r - c = 1$$

The numbers *n*, *b*, *r*, and *c* are the characteristic set for the molecule.[26] The characterization of the critical points allows the establishment of the molecular structure, as well as the study of the chemical bonds in unusual conditions, because the topological approximation does not show a difference between a normal (strong) bond and those resulting from weak interactions.[18,26−29]

Results and Discussions

For dimethylphosphinoyl(methylsulfanyl)methane (DMP-MSM **1**, Scheme 1) three rotamers of gauche and anti conformers in the C−S−C−P segment were optimized at Becke3LYP/6-31G(*d*,*p*). All structures were minima with no negative eigenvalues and imaginary frequencies. The gauche conformer **1-*g***, where the oxygen atom points out toward the thiomethyl group, is the global minima, followed by **1′-*a*** and **1′-*g*** conformers, which have a common relationship: the P−O bond is antiperiplanar (*app*) to the C−S bond and the rotamers **1′′-*g***, **1-*a***, and **1′′-*a*** involve arrangements were the P−O bond is antiperiplanar (*app*) to C−H bonds. The **1′′-*g*** conformer is more energetic (3.9 kcal/mol) than **1-*g***. This is despite the fact the C−P bond is *app* to a sulfur lone pair and goes against the expected $n_S \rightarrow \sigma^*_{C-P}$ stabilizing stereoelectronic interaction (Figure 2).

The geometry of these rotamers is reported in Table 1. No $n_S \rightarrow \sigma^*_{C-P}$ stereoelectronic participation is supported by these data. This is in agreement with experimental results[1,2] because no C−S contraction and C−P elongation was determined.

Frequency calculations include thermochemistry analysis of the system. This allows one to calculate zero-point energy, enthalpy, and entropy, values that are included in Scheme 1. Enthalpy contributions follow the same energetic tendencies of the total energy and are not scaled. It can be observed that the **1-*g*** conformer has the lower degree of freedom.

In the case of 1,3-dithiane derivatives, all isomers maintain a chair conformation. As summarized in Table 2 and Scheme 2, the axial conformer **2-*ax*** is estimated to be 4.45 kcal/mol more stable than **2-*eq***. In **2-*ax*** the P−O group points toward the center of the ring, the methyl-inside rotamer **2′-*ax*** being 6.37 kcal/mol higher in energy. By contrast, in the equatorial conformer **2′-*eq*** the P−O bond is antiperiplanar to the C−S bond and it is 1.38 kcal/mol more stable than **2-*eq***, which is the conformer observed experimentally. Inclusion of zero-point

Table 1. Geometry at the B3LYP/6-31G(*d*,*p*) Level of Conformers of Dimethylposphinoyl(methylsulfanyl)methane (**1**)[a]

	1-*g*	**1′-*g***	**1′′-*g***	**1-*a***	**1′-*a***	**1′′-*a***
C_3-S	1.834	1.838	1.838	1.833	1.834	1.833
C_3-P	1.850	1.853	1.854	1.852	1.851	1.852
$S-C_1$	1.832	1.828	1.828	1.827	1.827	1.827
P−O	1.504	1.502	1.500	1.499	1.501	1.499
$P-C_6$	1.828	1.831	1.830	1.830	1.829	1.830
$P-C_7$	1.835	1.830	1.836	1.835	1.829	1.835
C_1-S-C_3	100.7	101.3	100.8	99.1	99.7	99.1
S−C−P	114.3	118.3	115.4	111.8	115.3	111.8
C−P−O	113.9	111.7	114.0	114.7	111.3	114.7
$C-P-C_6$	104.7	106.2	105.7	104.6	105.2	104.6
$C-P-C_7$	103.5	104.4	102.8	102.3	105.2	102.3
C−S−C−P	72.0	95.8	100.4	166.5	179.8	166.3
S−C−P−O	60.0	177.6	67.9	58.8	179.9	56.7
$S-C-P-C_6$	65.9	52.3	58.6	69.7	55.4	69.8
$S-C-P-C_7$	175.9	57.9	168.2	178.8	55.3	179.0

[a] See Scheme 1 for numbering.

Table 2. Geometry at the B3LYP/6-31G(*d*,*p*) Level of Conformers of Dimethylposphinoyl-1,3-dithiane (**2**)[a]

	2-*ax*	**2′-*ax***	**2-*eq***	**2′-*eq***
S_1-C_2	1.840	1.839	1.839	1.843
C_2-S_3	1.840	1.844	1.839	1.839
S_3-C_4	1.844	1.838	1.839	1.837
C_4-C_5	1.531	1.529	1.532	1.530
C_5-C_6	1.531	1.529	1.532	1.530
C_6-S_1	1.844	1.837	1.838	1.838
C_2-P	1.869	1.879	1.874	1.876
P−O	1.506	1.500	1.479	1.499
$P-C_9$	1.831	1.832	1.831	1.830
$P-C_{10}$	1.831	1.832	1.832	1.827
$S_1-C_2-S_3$	114.1	115.5	113.7	114.3
$C_2-S_3-C_4$	100.5	103.3	98.0	99.0
$S_3-C_4-C_5$	113.9	114.5	114.3	115.0
$C_4-C_5-C_6$	113.6	113.2	114.0	113.7
$C_5-C_6-S_1$	113.9	114.7	114.2	114.3
C_6-S-C_2	100.5	102.9	98.0	99.5
S_1-C_2-P	112.3	113.9	110.1	112.2
S_3-C_4-P	112.3	117.3	110.8	108.8
C_2-P-O	113.3	111.8	115.1	112.2
C_2-P-C_9	104.8	108.1	103.4	104.1
C_2-P-C_{10}	104.8	103.8	103.0	105.1
$S_1-C_2-S_3-C_4$	56.4	47.4	61.8	58.3
$C_2-S_3-C_4-C_5$	57.8	54.2	59.0	58.2
$S_3-C_4-C_5-C_6$	66.9	66.7	65.5	65.9
$C_4-C_5-C_6-S_1$	66.9	67.5	65.7	65.5
$C_5-C_6-S_1-C_2$	57.8	55.2	59.3	58.1
$C_6-S_1-C_2-S_3$	56.4	48.6	61.9	58.6
S_1-C_2-P-O	66.1	50.5	60.6	175.5
S_3-C_2-P-O	66.1	170.1	66.0	57.0
$C_4-S_3-C_2-P$	72.9	90.4	173.6	175.3
$C_6-S_1-C_2-P$	72.9	91.5	173.1	176.8
$S_1-C_2-P-C_9$	169.7	75.8	173.5	51.8
$S_1-C_2-P-C_{10}$	60.1	173.5	64.8	59.8

[a] See Scheme 2 for numbering.

Scheme 2. Total Energy (TE, hartrees), Relative Total Energy (RTE, kcal/mol), Zero-Point Energy (ZPE, hartrees), Enthalpy (*H*, hartrees), and Entropy (*S*, eu) of C−P Rotamers of Dimethylphosphinoyl-1,3-dithiane at B3LYP/6-31G(*d*,*p*)

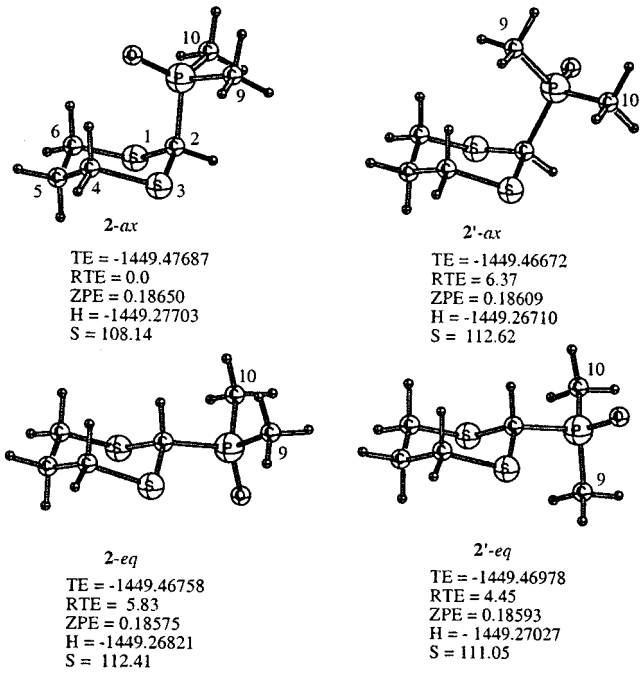

Scheme 3. Expected Dominant Stereoelectronic Interactions in **2-*ax*** and **2-*eq***

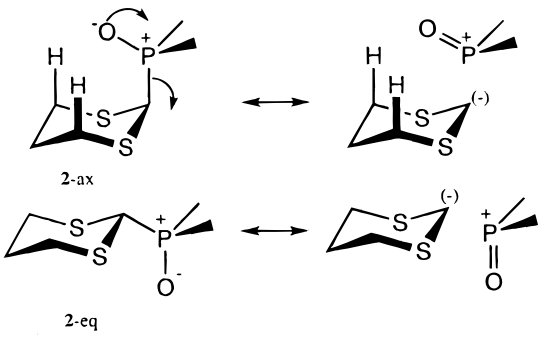

energy, thermal energies, and thermal enthalpies preserves energetic trends. Experimental $\Delta H°$ and $\Delta S°$ values of diphenylphosphinoyl-1,3-dithiane are 2.21 kcal/mol and 4.27 eu, respectively, and these values are in good agreement with values calculated in this study: 4.24 kcal/mol and 2.9 eu.[30]

Because of the polar nature of the P−O bond, high charge concentration is expected at the oxygen atom, giving rise to electrostatic interacions with proximal hydrogen atoms. On the other hand, a dominant $n_O \rightarrow \sigma^*_{C-P}$ stabilizing hyperconjugative interaction is expected (Scheme 3) over $n_S \rightarrow \sigma^*_{C-P}$ because of the better donor properties of oxygen.

Hyperconjugation appears not to be a plausible answer for the conformational preference of **2-*ax***. If $n_S \rightarrow \sigma^*_{C-P}$ would be a dominant hyperconjugative interaction the energetic differences between **2-*ax*** and **2′-*ax*** would be smaller due only to steric repulsion between the methyl group and the 4,6-*syn*-diaxial hydrogens. An extra stabilizing factor would be present in **2-*ax***. Interestingly the entropy term of this conformer is smaller with respect to the others, as a consequence of

(30) Juaristi, E.; Cuevas, G. *Tetrahedron Lett.* **1992**, *33*, 2271. Juaristi, E.; Cuevas, G. *J. Am. Chem. Soc.* **1993**, *115*, 1313.

Scheme 4. Gauche-Gauche and Axial-Gauche Conformations of **1**−**4**

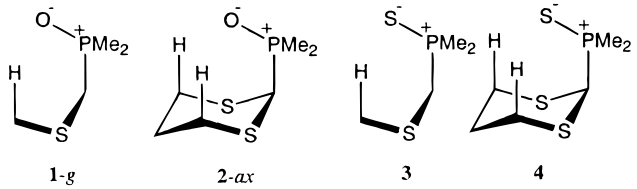

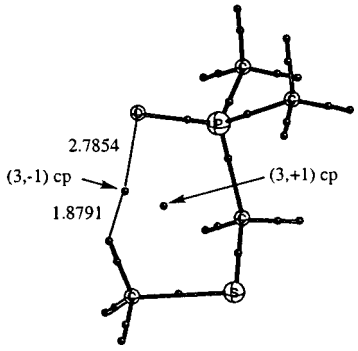

Figure 3. Relevant ring and bond critical point in **1-*g***. Distances between atoms and bond critical points are in au.

restrictions in rotational freedoms related to some interaction with 4,6-*diaxial*-hydrogens.

The fact that conformers displaying oxygen pointing toward the hydrogen atoms in the α position with respect to sulfur are lower in energy implies a stabilizing factor that could be studied through the atoms in molecules approach by the rigorous interpretation of the electronic density. Single-point calculations of **1-*g***, **2-*ax***, and their thiophosphinoyl derivatives were performed at the B3LYP/6-31G(*d*,*p*)//(BP + NLSCF/DZVP2) level (Scheme 4).[19]

In Figure 3, a bond path and critical point of order (3,−1) are shown, corresponding to DMP-MSM (**1-*g***). The bond path ends in the oxygen atom of the phosphoryl group and the next hydrogen atom. This bond generates an annular system, thus requiring the existence of a critical ring point type (3,+1) to satisfy the Poincare−Hopf relationship. Properties of the related critical points are shown in Table 3.

The electronic density of a critical point of a weak bond is twenty times less than the density of a critical point in a normal C−H bond. These results agree with those reported by Cioslowski for weak bonds in charge-transfer complexes.[18] The properties of the hydrogen molecule at the same level of theory for comparison purposes are shown in the same table.

The positive value of $\nabla^2\rho$ (ρ) (which is equal to the sum of three curves of ρ) on the critical bond point is related to the interaction of closed-shell systems, ionic bonds, hydrogen bonds, and van der Waals bonds, to which a notable ionic character may be assigned.[31,32]

The total path length and the geometric distance between the linked atoms are shown in Table 4. One may observe that the bond path is curved or, in other words, the bond path is longer than the geometric distance of the atoms involved.

The thiophosphorylated derivative (**3**, Scheme 4) has a similar critical points distribution with respect to **1-*g*** as depicted in Figure 3 and in Tables 3 and 4 where the properties of the relevant critical points and their bond paths are included. This system is analogous to **1-*g***. It was possible to characterize the

(31) Kremer, D.; Kraka, E. *Croat. Chem. Acta* **1984**, *57*, 1265.
(32) Bader, R. F. W.; Tal, Y.; Anderson, S. G.; Nguyen-Dang, T. T. *Isr. J. Chem.* **1989**, *19*, 3234.

Table 3. Critical Points Related to Weak Interaction in **1-*g***, **2-*ax***, and **3**−**6** (in au)

compd	signature	$\rho\times10^2$	$\nabla^2\rho\times10^2$	$\lambda^a\times10^2$	$\lambda^a\times10^3$	$\lambda^a\times10^3$	ϵ
1[b]	3,−1	1.095	3.541	−1.046	−9.577	5.545	0.0922
1[b]	3,+1	0.691	3.172	−3.867	−10.494	2.509	
2-a[c]	3,−1	10.897	3.525	−10.061	−9.414	5.473	0.0688
2-b[c]	3,−1	10.203	3.345	−9.224	−8.567	5.128	0.0766
2-c[c]	3,+1	11.801	6.442	−6.043	35.206	3.526	
2-d[c]	3,+1	5.377	2.266	−2.713	12.229	1.315	
2-e[c]	3,+1	7.071	3.193	−3.632	10.398	2.517	
2-f[c]	3,+1	6.865	3.074	−3.522	9.698	2.456	
2-g[c]	3,+3	4.849	2.157	4.140	6.661	1.077	
3[b]	3,−1	1.020	3.056	−8.056	−7.729	4.637	0.0467
3[b]	3,+1	0.598	2.278	−0.249	−8.334	1.694	
4-a[c]	3,−1	8.795	2.612	−6.498	−1.157	3.878	0.0553
4-b[c]	3,−1	8.625	2.561	−6.321	−5.979	3.791	0.0573
4-c[c]	3,+1	11.623	6.325	−6.015	34.353	3.491	
4-d[c]	3,+1	4.597	1.555	−2.041	8.422	0.917	
4-e[c]	3,+1	5.764	2.087	−2.298	7.076	1.609	
4-f[c]	3,+1	5.708	2.059	−2.277	6.940	1.593	
4-g[c]	3,+3	4.122	1.511	3.268	4.605	7.231	
5-a[c]	3,−1	8.711	2.897	−7.351	−6.268	4.259	0.1728
5-b[c]	3,−1	8.522	2.844	−7.122	−6.004	4.156	0.1862
5-c[c]	3,+1	16.660	10.568	−1.315	5.759	6.124	
5-d[c]	3,+1	4.645	1.912	−0.299	8.675	1.082	
5-e[c]	3,+1	7.107	3.129	−4.578	7.694	2.818	
5-f[c]	3,+1	7.052	3.093	−4.550	7.352	2.813	
5-g[c]	3,+3	4.645	1.945	0.314	8.319	1.082	
6-a[c]	3,−1	8.849	2.535	−5.975	−5.422	3.674	0.1021
6-b[c]	3,−1	8.515	5.323	−5.993	−5.450	6.680	0.0995
6-c[c]	3,+1	16.133	10.134	−12.897	55.984	5.845	
6-d[c]	3,+1	4.366	1.546	−0.387	6.549	0.930	
6-e[c]	3,+1	6.491	2.470	−3.310	7.289	2.078	
6-f[c]	3,+1	6.509	2.480	−3.348	7.330	2.082	
6-g[c]	3,+3	4.364	1.583	0.424	6.182	0.923	
H−H	3,−1	26.834	−134.347	−24.117	−24.117	146.469	0.0

[a] Eigenvalues of the Hessian at cp. [b] See Figure 3 for numbering. [c] See Figure 4 for numbering.

Table 4. Bond Trajectories (in au) of **1-*g***, **2-*ax***, and **3**−**6**

molecule	trajectory[a]	total bond path (*a*)	geometric bond length (*b*)	diff $a-b$
1-*g*		4.7049	4.6524	0.0525
2-*ax*	a	4.7261	4.6745	0.0516
2-*ax*	b	4.7988	4.7422	0.0566
3		5.3072	5.2735	0.0337
4	a	5.4933	5.4546	0.0387
4	b	5.5169	5.4771	0.0398
5	a	5.0146	4.9456	0.0690
5	b	5.0403	4.9699	0.0704
6	a	5.6190	5.5494	0.0696
6	b	5.6137	5.5460	0.0677

[a] See Figures 3 or 4 for numbering.

critical ring point to fulfill the topological relation associated with the existence of point (3,−1).

Between these two systems, the ellipticity varies considerably, and although the bond is longer, the difference in the total length of the S−H bond and the geometric distance is smaller (see Table 4). Finally, the difference in density suggests that the interaction is stronger with oxygen as an acceptor atom than with sulfur. Upon analysis of the curvatures, one may deduce the existence of a certain electronic delocalization along the path.

A gradient vector field map of the electron density in the average plane containing the P−O···H−C segment of molecule **1-*g*** is included in Chart 1. Each nucleus acts as an attractor and the region of space spanned by the trajectories that terminate

Chart 1

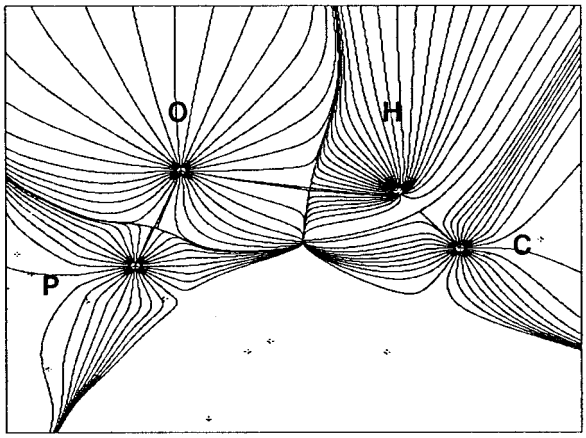

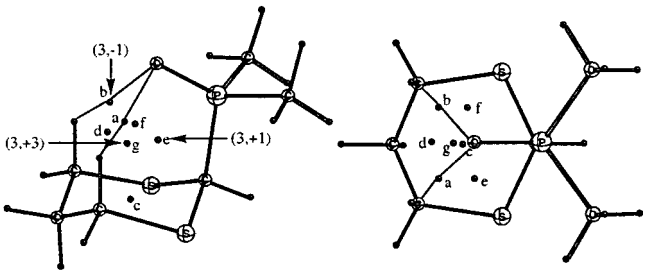

Figure 4. (3,-1), (3,+1), and (3,+3) critical points in **2-*ax*** associated with weak interactions in different views.

at a given nucleus define its atomic basin. The (3,−1) critical point serves as the origin for the unique pair of trajectories that define the bond path and as the terminus for the trajectories of the two-dimensional manifold defining the zero-flux surface.

The axial DMP-DT (**2-*ax***, Figure 4) constitutes a more interesting case because the results suggest the participation of two hydrogen bonds. As a result of the annular closure, one may observe an adamantane-like system. The new rings require the existence of three critical points of type (3,+1) as well as the critical 1,3-dithiane ring point. Furthermore, this group of rings and their critical points upon closure of a cage require the existence of a critical cage point (3,+3). The total of these critical points was determined and their properties are shown in Table 3. Table 4 includes the properties of the bond paths involved.

It is interesting to point out that for this molecule, the density (ρ) and the Laplacian of ρ of one of the bond paths are similar to those of the acyclic related compound (**1-*g***), while the other is smaller. The ellipticity of both paths is smaller and suggests electronic delocalization.

This result, together with the fact that the oxygen atom is closer to the critical point of highest density (ρ) values (the optimization of the geometry was achieved without considering geometric or symmetric restrictions), suggests that one of the hydrogen bridges is stronger than the other, as proposed before.[2,4,33] The bond path is 4.726 au and the dihedral angle P−O−Hax−C is 32.7° for the stronger bond and 4.799° with a dihedral angle of 43.0° for the other path. The highest value of $\nabla^2\rho$ for the strongest bond implies the electrostatic nature of the interaction.[32]

Finally, the properties of the critical point of order (3,+1) of the 1,3-dithiane ring (point c in Figure 4) show higher values

(33) Mikolajczyk, M. *Pure Appl. Chem.* **1987**, *59*, 983. Mikolajczyk, M.; Graczyk, P. P.; Wieczorek, M. W.; Bujacz, G. *Tetrahedron* **1992**, *48*, 4209.

Scheme 5. Stereoelectronic Involvement of Sulfur Atoms in **2-*ax***

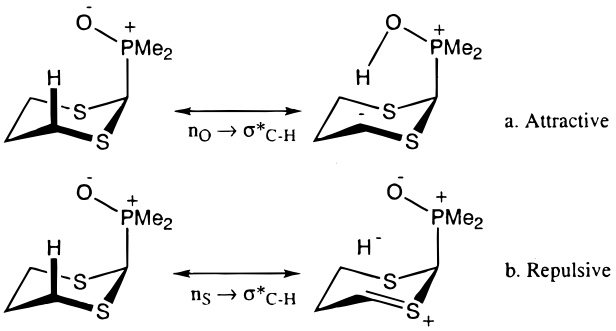

of ρ, $\nabla^2\rho(r)$, and λ than the critical points of the same order originating from weak interactions (points d, e, and f in Figure 4). From among these three points the weakest is that with two components originating from the H···O interactions (point d). The comparison of these values suggests the possibility of topologically differentiating weak interactions from normal bonds.

The last heterocyclic system under study is the 1,3-dithiane substituted by the thiophosphoryl group (**4**). In this case, all the critical points required to characterize this structure were determined and shown in Table 3. Their geometric pattern is similar to that shown in Figure 3 for **2-*ax***.

Density and the Laplacian of density are substantially smaller than those values observed for the open chain system; nevertheless, the ellipticities are larger. Again, the strong bond belongs to the one closest to the sulfur atom (path bond lengths 5.493 au vs 5.517 au and dihedral angles P−S−Hax−C of 28.6° vs 29.2° for the weaker).

The global diminution of ρ and $\nabla^2\rho(r)$ with respect to the open chain analogue would be the result of the steric size of the sulfur atom, which provokes a strong repulsion with the hydrogen atoms (in the system with the P−O group, one can also observe smaller values of this properties, but to a smaller degree). Moreover, the strong dependence of $\nabla^2\rho(r)$ on the molecular geometry (which also causes changes in the interatomic distance) suggests the electrostatic nature of the interaction.[26,32]

From the molecular systems considered until now, one can expect that stereoelectronic effects are important and determine where the 1,3-dithiane's heteroatoms can actively participate. Pauling's electronegativity of the sulfur is 2.58, very similar to that of the carbon: 2.55. If the interaction H···X (X = O, S) has an electrostatic nature, the properties of the critical points of the dithiane or cyclohexane derived compounds should be similar (Scheme 5). But if a $n_O \rightarrow \sigma^*_{X-H}$ interaction is important, this should be even stronger in 1,3-dithiane due to sulfur's capacity for stabilizing carbanions in the α position (Scheme 5a). One should also consider that the $n_S \rightarrow \sigma^*_{C4,6-Hax}$ interaction can diminish the donating capacity of the C−H group.

To determine the role of the sulfur endocyclic atom in these interactions, an optimization of the geometry of the carbocyclic analogues of **2-*ax*** and **4** was made. Properties of relevant critical points are shown in Table 3 for dimethylphosphinoyl- (**5**) and dimethyltiophosphinoylcyclohexane (**6**).

Sulfur substitution by methylene groups in **2-*ax*** (see Figure 4 since topology is similar) produces an important change in the molecular geometry, shortening the distance H_{ax}−O. As a result, the bonding paths and the bond lengths are minor; nonetheless, differences between them are larger because bonds are more curved (see Table 4).

Table 5. Geometrical Parameters of **5** and **6** (in deg)

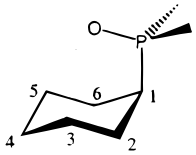

angle	X = O	X = S
$C_6-C_1-C_3$	111.04	114.45
$C_6-C_1-C_2-C_3$	50.69	49.15
C_2-C_1-P-X	62.30	64.40
$C_3-C_2-C_{1-P}$	76.00	82.23

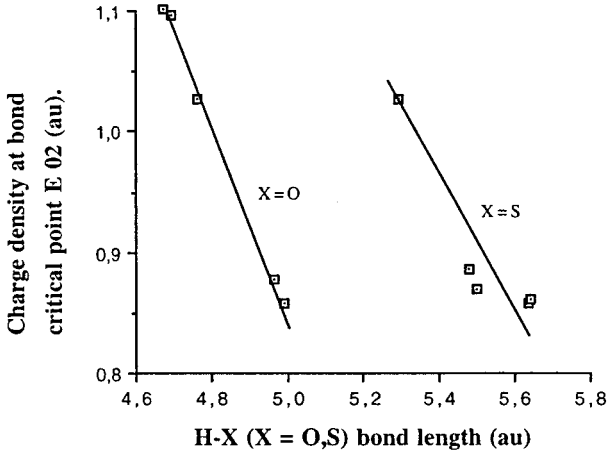

Figure 5. Relationship between H−X (X = O, S) distance in compounds **1**−**6** and density at bond critical points.

On the other hand, properties of the critical points show that the weaker interactions cannot be explained merely in electrostatic terms (if we consider only the difference in electronegativity and distance between interacting nucleus and, therefore, minor distance, stronger interaction). One has also to consider the participation of stereoelectronic effects in that interaction.

Stereoelectronic interactions modify the charge distribution (Scheme 5) and the substitution modifies the distance between atoms.

The case of compound **6** (Table 3) is interesting because the steric requirements of the thiophosphinoyl group are larger than those of the phosphinoyl group and the cyclohexane chair is deformed, especially in the segment $C_6-C_1-C_2$, where it is flattened. The relevant angles are shown in Table 5. This deformation allows the sulfur atom to take the better position to keep a maximal electrostatic interaction, with the minimum steric repulsion.

This fact could explain the high values in the density shown by this molecule in its critical points. The relationship between the critical bond points and the hydrogen bond distance is linear for the phosphoryl group (P−O). This linearity is poor for the sulfur analogue, probably due to steric reasons (Figure 5).

Conclusions

The topological properties of the gauche-gauche conformers of the dimethylphosphinoyl- (**1-*a***) and dimethylthiophosphinoyl-(methylsulfanyl)methane (**3**), and in the axial-gauche conformers of the same substituting groups in 1,3-dithiane (**2-*ax*** and **4,** respectively), were characterized at the Becke3LYP/6-31G(*d,p*)//(BP+NLSCF)/DZVP2 level. From the calculated density,

X···H (X = O, S) bond trajectories showed the existence of interactions of the hydrogen bond type in these molecules.

It is important to point out that the conditions simulated in this calculation favor these interactions (isolated molecule, 0 K and in the gas phase). The interactions H−X (X = O, S) are characterized as having a small value of ρ, a small and positive value of $\nabla^2\rho(r)$, as well as a strong dependence with respect to the annular substituent.

There is no doubt about the existence of additional bond paths in the calculated density. The weak interactions have associated, larger ellipticity values and bond curvatures. The fact that the properties of the critical points, generated by weak interactions, are less than those originated by normal interactions allows for its differentiation.

When the atom bound to phosphorus is oxygen, the relationship between the densities of the points (3,−1) and the length of H···O bonds is linear. Linearity remarkably diminishes in the thiophosphinoyl case, probably due to steric reasons. Finally, this type of interaction can contribute as a stabilizing factor to the anomeric effect shown in these systems.

Acknowledgment. I am deeply grateful to Prof. Dr. R. W. F. Bader for a copy of the AIMPAC package of programs and to Dr. Rebeca López-García and Q.F.B. Julieta Tenorio-Llano for careful revision of this manuscript. I would like to thank the Alexander von Humboldt Foundation and the Consejo Nacional de Ciencia y Tecnología (CONACYT) for financial support via grant 32420-E. I also want to thank the Dirección General de Servicios de Cómputo, Universidad Nacional Autónoma de México (DGSCA; UNAM) for computational support and a generous gift of Cray-Y-MP464 CPU time and Prof. Eusebio Juaristi, Prof. Guillermo Delgado, Prof. Alberto Vela, Prof. Barbara Gordillo, Prof. Luis Angel Maldonado, and Angel Fernando Olvera Klessa for their stimulating comments on this study.

JA9731231